Electron-capture dynamics in collisions of Si^4 ions with He atoms at intermediate energies

R. Suzuki

Computer Center, Hitotsubashi University, Tokyo 186-8603, Japan

A. Watanabe and H. Sato

Department of Information Sciences, Ochanomizu University, Tokyo 112-8610, Japan

J. P. Gu, G. Hirsch,[†] and R. J. Buenker

Theoretische Chemie, Bergische Universität-Gesamthochschule Wuppertal D-42097, Wuppertal, Germany

M. Kimura

Graduate School of Science and Engineering, Yamaguchi University, Ube 755-8611, Japan

P. C. Stancil

Department of Physics and Astronomy, University of Georgia, Athens, Georgia 30602-2451

Electron capture resulting from collisions of Si^{4+} ions with He atoms below 25 keV/u is investigated using a molecular-orbital representation within both the semiclassical and quantal representations. Nine molecular states connecting both to single and double electron-capture processes are included, and hence radial and rotational couplings among these channels are fully considered. Electronic states and corresponding couplings are determined by the multireference single- and double-excitation configuration interaction method. The present results tie in well with the earlier calculations of Stancil *et al.* at lower energies, but show a rather different magnitude from the theoretical results of Bacchus-Montabonel and Ceyzeriat and are somewhat smaller than the measurements of Tawara *et al.* The present rate constants do not support the experimental finding of Fang and Kwong at 4,600 K.

I. INTRODUCTION

Electron capture due to collisions of multiply charged ions with neutral species plays an important role in a variety of astrophysical and laboratory plasmas. The process can affect the ionization balance of the plasma and is a mechanism for populating excited states of the product ion [1]. The particular reaction

$$\text{Si}^{4+} + \text{He} \rightarrow \text{Si}^{3+} + \text{He}^+ \qquad (1)$$

has been studied via a number of theoretical investigations and may be important in planetary nebulae and astrophysical shocks [2–4]. Cross sections for process (1) have been computed using the molecular-orbital close-coupling (MOCC) approach with both quantum-mechanical [4,5] and semiclassical [6] descriptions of the nuclear motion. The various calculations are in fair agreement, though discrepancies as large as a factor of 2 are evident in certain energy ranges. Experimental studies have been limited to a recent total cross section measurement [7] and a determination of the rate coefficient [8]. The cross sections measured by Tawara *et al.* [7], though over a limited energy range, are in fair agreement with all calculations. However, Fang and Kwong [8], who measured the rate coefficient at 4600 K using an ion trap technique, obtained a result that is nearly two orders of magnitude smaller than the rate coefficients calculated with the Landau-Zener model [1] as well as those obtained from the quantum-mechanical MOCC results [4,5]. The experiment in Ref. [8], however, cannot resolve the various product channels and is limited to a single energy.

In this paper, we revisit this collision system in an attempt to resolve the discrepancies between experiment and theory. In addition to the reaction (1), the first semiclassical MOCC calculations are performed for the double-capture channel

$$\text{Si}^{4+} + \text{He} \rightarrow \text{Si}^{2+} + \text{He}^{2+}. \qquad (2)$$
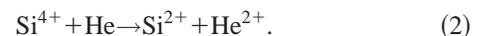
These calculations incorporate new adiabatic potentials and nonadiabatic coupling matrix elements computed with the multireference single- and double-excitation configuration-interaction (MRD-CI) method. Quantum-mechanical MOCC calculations are also performed at low energies to extend the previous work in Ref. [4]. Silicon ions have become increasingly important for applications such as Si-thin film manufacturing based on the ion-beam technology, and accurate information on cross sections for inelastic processes and their dynamics are highly desirable.

II. THEORETICAL MODEL

A. Molecular states

The adiabatic potential curves of SiHe^{4+} are obtained by employing the *ab initio* MRD-CI method [9], with configuration selection at a threshold of 1.0×10^{-7} hartree and en-

TABLE I. Number of reference configurations, N_{ref}, and number of roots, N_{root} treated in each irreducible representation and the corresponding number of generated (N_{tot}) and selected (N_{sel}) symmetry-adapted functions for a threshold of 1.0×10^{-7} hartree at Si-He internuclear distance of $2.0 a_0$ in the SiHe^{4+} calculation.

State	$N_{\text{ref}}/N_{\text{root}}$	N_{tot}	N_{sel}
$^1 A_1$	32/8	935 909	153 550
$^1 B_1$	11/3	432 392	65 274
$^3 A_1$	22/6	1 211 586	162 846
$^3 B_1$	10/3	665 882	89 542

ergy extrapolation, using the Table configuration interaction (CI) algorithm [10]. The two electrons in the first (lowest) molecular orbital (MO) are kept inactive in the present CI calculation, and the highest MO is discarded. The coupling matrix elements are calculated by using the resulting CI wave functions. The radial coupling elements are calculated by using a finite-difference method [11]. In the calculations, the basis set for the silicon atom is $(13s10p4d1f)$, which is contracted to $[10s7p4d1f]$ [12]. But the exponent of the f function is reoptimized and the value is 0.34; the s, p basis set is from Ref. [13], also see Ref. [14]. For the He atom, the $(10s5p1d)/[7s4p1d]$ basis set in Ref. [15] is employed, but the most diffuse d function with the exponent of 0.03 is deleted. Further details of our *ab initio* MRD-CI calculations are listed in Table I.

B. Scattering dynamics

1. Semiclassical approach

A semiclassical MO expansion method with a straight-line trajectory of the incident ion was employed to study the collision dynamics above 30 eV/u [16]. In this approach, the relative motion of heavy particles is treated classically, while electronic motions are treated quantum mechanically. The total scattering wave function was expanded in terms of products of a molecular electronic state and atomic-type electron translation factors (ETF's), in which the inclusion of the ETF satisfies the correct scattering boundary condition. Substituting the total wave function into the time-dependent Schrödinger equation and retaining the ETF correction up to the first order in the relative velocity between the collision partners, we obtain a set of first-order coupled equations in time. Transitions between the molecular states are driven by
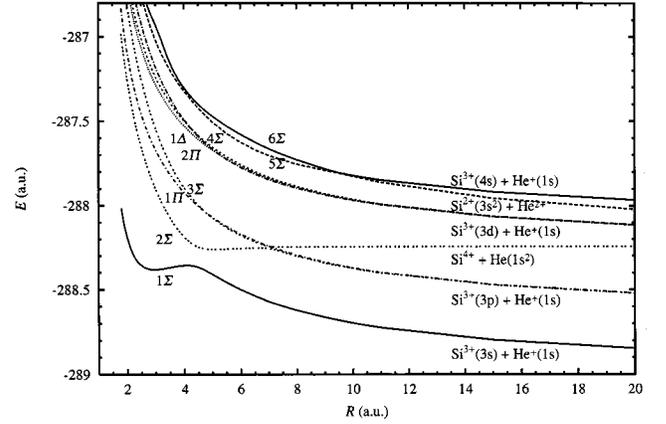
FIG. 1. Adiabatic ($^1\Sigma^+$, $^1\Pi$, $^1\Delta$) potentials for the SiHe^{4+} system.

nonadiabatic couplings. By solving the coupled equations numerically, we obtain the scattering amplitudes for the transitions; the square of the amplitude gives the transition probability, and integration of the probability over the impact parameter gives the cross section. Nine molecular states are included in the dynamical calculations (see Fig. 1) separating to the initial channel $[\text{Si}^{4+}+\text{He}(^1\text{S})](3\ ^1\Sigma^+)$, the single-capture channels $[\text{Si}^{3+}(^2\text{S})+\text{He}^+\!:\!1\ ^1\Sigma^+]$, $[\text{Si}^{3+}(^2\text{P})+\text{He}^+\!:\!2\ ^1\Sigma^+,1\ ^1\Pi]$, $[\text{Si}^{3+}(^2\text{D})+\text{He}^+\!:\!4\ ^1\Sigma^+,2\ ^1\Pi,1\ ^1\Delta]$, $[\text{Si}^{3+}(^2\text{S})+\text{He}^+\!:\!6\ ^1\Sigma^+]$, and the double-capture channel $[\text{Si}^{2+}(^1\text{S})+\text{He}^{2+}\!:\!5\ ^1\Sigma^+]$.

2. Quantum approach

A fully quantum-mechanical representation of the MO expansion method was employed for collision energies from 10 to 230 eV/u to extend the earlier work of Stancil *et al.* [4]. In this energy region, transitions are also driven by nonadiabatic coupling. The total scattering wave function is expanded as a sum of products of molecular electronic wave functions and nuclear wave functions. The coupled equations in R, that the nuclear wave functions satisfy, are obtained from the time-independent Schrödinger equation [16]. The coupled equations are solved numerically, after partial-wave decomposition, to obtain the scattering matrix. The molecular states included are three Σ channels: (1) $[\text{Si}^{4+}+\text{He}\!:\!3\ ^1\Sigma]$, $[\text{Si}^{3+}(^2\text{S})+\text{He}^+\!:\!1\ ^1\Sigma^+]$, and $[\text{Si}^{3+}(^2\text{P})+\text{He}^+\!:\!2\ ^1\Sigma^+]$.

TABLE II. The present molecular orbitals and corresponding asymptotes of SiHe^{4+}.

No.	Asymptote	Relative energy (cm^{-1})		State
		Exp.	Cal.	
1	$\text{Si}^{3+}(^2\text{S}_g)+\text{He}^+(^2\text{S}_g)$	0	0	$1\ ^1\Sigma^+$
2	$\text{Si}^{3+}(^2\text{P}_u)+\text{He}^+(^2\text{S}_g)$	71 290	71 181	$2\ ^1\Sigma^+,1\ ^1\Pi$
3	$\text{Si}^{3+}(^2\text{D}_g)+\text{He}^+(^2\text{S}_g)$	160 377	160 599	$4\ ^1\Sigma^+,2\ ^1\Pi,1\ ^1\Delta$
4	$\text{Si}^{4+}(^2\text{S}_g)+\text{He}(^1\text{S}_g)$	165 793	165 013	$3\ ^1\Sigma^+,$
5	$\text{Si}^{2+}(^1\text{S}_g)+\text{He}^{2+}$	168 968	169 808	$5\ ^1\Sigma^+$
6	$\text{Si}^{3+}(^2\text{S}_g)+\text{He}^+(^2\text{S}_g)$	193 982	193 158	$6\ ^1\Sigma^+$

TABLE III. The comparison of asymptotic energies for first three states.

State	Energy (a.u.)			
	Present	Ref. [4]	Ref. [6]	Expt. [16]
$Si^{4+}+He[3\ ^1\Sigma]$	0	0	0	0
$Si^{3+}(3p)+He^+[2\ ^1\Sigma]$	0.427 53	0.430 16	0.433 14	0.430 58
$Si^{3+}(3s)+He^+[1\ ^1\Sigma]$	0.751 85	0.755 22	0.745 81	0.755 41

III. RESULTS AND DISCUSSION

A. Adiabatic potentials and coupling matrix elements

The present adiabatic potential curves including single- and double-capture channels for Σ and Π states are illustrated in Fig. 1. The precision of the present calculations and asymptotes can be judged from Table II. Asymptotically the $4\ ^1\Sigma^+$ state corresponds to the initial $[Si^{4+}+He(^1S)]$ channel. However, it has a strong avoided crossing with the $3\ ^1\Sigma^+$ state at around $R=30$ a.u., and hence, inside of this R region, they switch with the $3\ ^1\Sigma^+$ state acquiring the character of the initial neutral channel. A simple Landau-Zener calculation suggests that this avoided crossing between the $3\ ^1\Sigma^+$ and $4\ ^1\Sigma^+$ channels can be safely treated as diabatic. Therefore we treat the $3\ ^1\Sigma^+$ channel as the initial channel in the present calculation. As a measure of the accuracy of the present calculation, the comparison of energies for the first three states with other theories along with experimental data [17] is made in Table III. All theories are found to be comparable in accuracy, but the results by Stancil *et al.* are found to be slightly better than any of these.

Representative coupling matrix elements both for the radial and rotational components are displayed in Figs. 2 and 3, respectively. Visual inspection suggests that most of the present relevant coupling matrix elements are in close agreement with those of other theories including that of Stancil *et al.* and Opradolce, McCarroll, and Valiron [5]. Couplings that connect to higher single- and double-capture states are found to be fairly strong, and hence it is important to assess the role of the double-capture process.

FIG. 3. Representative rotational coupling matrix elements between $^1\Sigma^+$ and $^1\Pi$ states.

B. Electron capture cross sections

1. Single capture

Partial cross sections for capture to the $1\ ^1\Sigma^+$, $2\ ^1\Sigma^+$, and $1\ ^1\Pi$ channels are shown in Fig. 4. Two main features are apparent: (i) the cross section for the $1\ ^1\Sigma^+$ states dominates above 200 eV/u while those for the $2\ ^1\Sigma^+$ and $1\ ^1\Pi$ states take over below this energy and begin to show an increasing trend as the energy lowers, and (ii) a strong oscillatory structure can be seen in the cross section for the $1\ ^1\Sigma^+$ state, while much weaker undulations are observed for the $2\ ^1\Sigma^+$ state. The oscillatory structure in the $1\ ^1\Sigma^+$ state is due to the extremum in the potential difference between the $1\ ^1\Sigma^+$ and $3\ ^1\Sigma^+$ states [18]. Although the $2\ ^1\Sigma^+$ state is present in-between, it is found to be diabatic in nature in the energy region where the oscillation can be seen, and hence the role of the $2\ ^1\Sigma^+$ state is secondary. As the collision energy becomes lower, however, the $2\ ^1\Sigma^+$ state increasingly becomes adiabatic, and the coupling between the $1\ ^1\Sigma^+$ and $2\ ^1\Sigma^+$ states becomes effective. Consequently this effect translates into the $2\ ^1\Sigma^+$ cross section, hence causing the out-of-phase oscillation. The effect of the $[Si^{3+}(^2D)+He^+;4\ ^1\Sigma^+,2\ ^1\Pi,1\ ^1\Delta]$ channels are very small

FIG. 2. Representative radial coupling matrix elements between $^1\Sigma^+$ states.
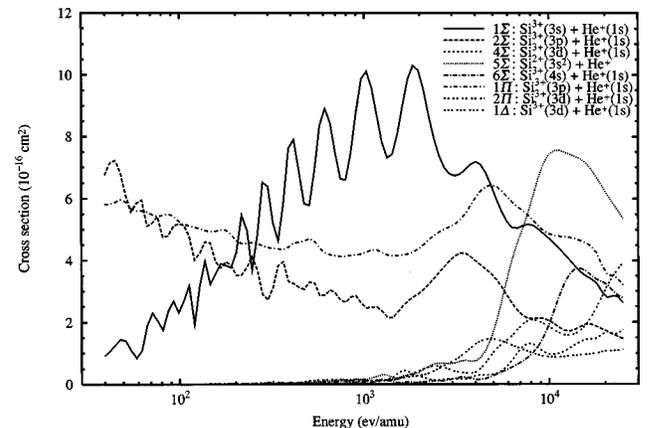
FIG. 4. Partial cross sections for single- and double-electron capture into each individual molecular channel from the semiclassical MOCC calculations.
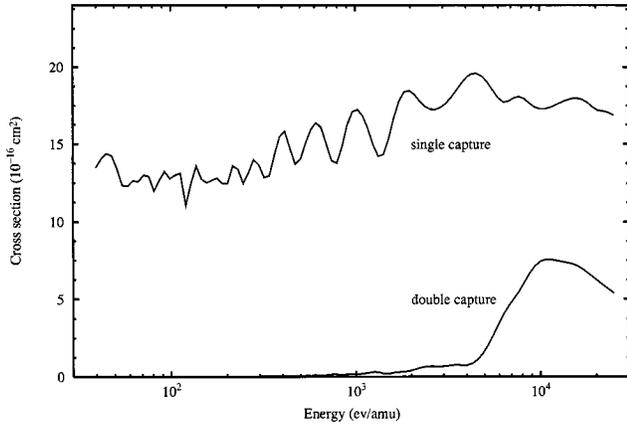
FIG. 5. Single- and double-capture cross sections in the collision energy from 40 to 25 keV/u from the semiclassical MOCC calculations.

FIG. 6. Single electron capture and double electron capture cross sections from the present quantum and semiclassical MOCC calculations in comparison to other theoretical and experimental results.

below 3 keV/u, but it becomes increasingly conspicuous as the energy increases. Obviously, these channels have a non-negligible effect above a few keV/u, and hence should be included in the theory. The contribution from the $1\ ^1\Delta$ state, however, is the smallest within the manifold.

2. Double capture

Double-capture cross sections are also included in Fig. 4. The size of the double-capture cross section is similar to that of $[Si^{3+}(^2D)+He^+]$ formation. Therefore, the flux promotion to this channel is expected to proceed through intermediate single-capture channels, i.e., the ladder-climbing model, below about 4 keV/u, hence increasing in the same manner and having a sizable cross section. However, as the energy increases further, the direct excitation to this channel begins to contribute, and this is exemplified by the rapid rise of the cross section that becomes dominant above 4 keV/u. A weak oscillatory structure is due to multichannel interference. At the highest end of the present energy range, double capture to excited states may become important, and hence, the present calculation may underestimate the double-capture processes.

3. Total cross sections

Total single- and double-capture cross sections are illustrated in Fig. 5. The single-capture cross section reaches its minimum with a value of 1×10^{-15} cm^2 at around 100 eV/u, and at both sides of the energy, it shows an increasing trend. It peaks at around 5 keV/u with a value of 2×10^{-15} cm^2, followed by a sharp decrease on the higher-energy side. The undulation due to the $1\ ^1\Sigma^+$ state is still apparently visible above the minimum although it significantly weakens below the minimum. The double-capture cross section is small, on the order of 10^{-18} cm^2 below 1 keV/u, but begins to increase, reaching about 5×10^{-16} cm^2 at 10 keV/u. It also shows small structures as described above. In the present energy region considered, the double-capture process is a secondary effect, but amounts to about 22% of the total capture at 30 keV/u.
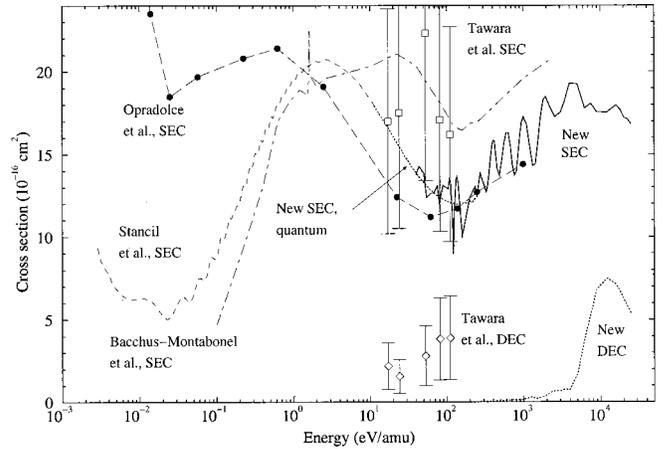
C. Comparison with other theories and experiments

In Fig. 6, all theoretical results including the present result are displayed along with the recent experimental data by Tawara *et al.* [7]. The present results are found to fit in very well with the previous quantum-mechanical MOCC result of Stancil *et al.* [4], which are extended here from 10 to 230 eV/u, to overlap the energy region of the present semiclassical calculation. The result by Opradolce, McCarroll, and Valiron [5] also appears to agree well above 100 eV/u, although their cross section below this energy is found to be smaller by 15% than that of Stancil *et al.*, down to 1 eV/u. However, the result of Opradolce, McCarroll, and Valiron has a peak at around 1 eV/u and slightly decreases below 1 eV/u, reaching a minimum at 0.02 eV/u, followed by a sharp increase for lower energies. This feature in the low-energy region is quite different from that of Stancil *et al.* The results of Bacchus-Montabonel and Ceyzeriat [6] are found to be in reasonable accord with that of Stancil *et al.* below 2 eV/u. However, their result continues to increase slowly above 2 eV/u and reaches a maximum at around 50 eV/u, while that of Stancil *et al.* already shows the decreasing trend beyond 2 eV/u with the present quantum MOCC results smoothly connecting to the present semiclassical MOCC results at 70 eV/u. Hence the present result does not agree with that of Bacchus-Montabonel and Ceyzeriat in magnitude, with theirs being larger by 50%, although the energy dependence for both results is found to be in fair agreement above 20 eV/u. Further, we have extended the calculation to lower energies using a three-channel approximation to estimate the rate coefficients, and have found good agreement with earlier results of Stancil *et al.* In order to understand the origin of this discrepancy, we have compared closely the three sets of adiabatic potentials and dominant coupling matrix elements reported by Bacchus-Montabonel and Ceyzeriat, by Stancil *et al.*, and from the current paper. As described earlier and seen in Table III, the precision of the adiabatic potentials for two dominant capture channels among the three theories are comparable with the maximum difference being less than 1% for both channels. The radial coupling between the $3\ ^1\Sigma$ and

$2\ ^1\Sigma$ states is dominant, and is considered to be the most important for the removal of flux. The magnitude of this coupling at the peak by Stancil *et al.* is found to be the largest, by about 6%, among the three. The peak height by Bacchus-Montabonel and Ceyzeriat appears to be the smallest, while that obtained in the current paper lies in the middle, which may be due in part to the effect of the type of ETF's used. The difference for the peak position of this coupling for the three theories is found to be insignificant. Although the visual inspection of adiabatic potentials and couplings does not provide strong evidence for the discrepancy, it is known, however, that small differences in the coupling often cause sizable differences in cross-section calculations, and this may be the source.

Very recently, Tawara *et al.* [7] measured single- and double-capture cross sections in the energy region from 20 to 100 eV/u. Their results have relatively large error bars, but the lowest two points agree better with that of Stancil *et al.*, while the three points at higher energies seem to agree with that of Bacchus-Montabonel and Ceyzeriat, being somewhat larger than the current semiclassical MOCC calculations. The experimental result does not resolve this discrepancy in the present case. They also measured double-capture cross sections, which are larger than the present results. Since the present calculation neglects double-capture channels to excited states, it may underestimate the total double-capture cross section. However, for collision energies less than 100 eV/u, capture to the Si^{2+} ground state should be the dominant channel. It is possible that the experimental data overestimates double capture, particularly since the double-capture threshold is 0.1 eV/u.

D. Rate coefficients

Rate coefficients for the process (1) have been evaluated by averaging the cross section over a Maxwellian velocity distribution from 5000 to 5×10^5 K. The present rate coefficients are found to gradually vary from 5.2×10^{-10} to 2.1×10^{-8} cm^3/s at the corresponding temperatures. Our rate coefficient at 5000 K is two orders of magnitude larger than the experimental data reported by Fang and Kwong [8] who gave a value of 4.54×10^{-12} cm^3/s. The present rate coefficients are consistent with those of Stancil *et al.*

IV. CONCLUSION

We have investigated single- and double-capture dynamics in collisions of Si^{4+} ions with He atoms in the energy region from 10 to 25 keV/u. The present results for single-capture cross section are found to agree very well with the previous result of Stancil *et al.* in the entire energy region studied. The results of Bacchhus-Montabonel and Cyzeriat are larger by 50% above 20 eV/u, although their energy dependence is in fair agreement with the present results above 20 eV/u. The experimental data by Tawara *et al.* for single capture is in good agreement with all the theoretical studies, but the error bars are too large to discriminate between the various calculations. As in the previous theoretical investigations, the current paper suggests that the rate coefficient measurement of Fang and Kwong is two orders of magnitude too small.

[1] S. E. Butler and A. Dalgarno, Astrophys. J. **241**, 838 (1980).

[2] R. E. S. Clegg, J. P. Harrington, M. J. Barlow, and J. R. Walsh, Astrophys. J. **314**, 551 (1987).

[3] S. E. Butler and J. C. Raymond, Astrophys. J. **240**, 680 (1980).

[4] P. C. Stancil, B. Zygelman, N. J. Clarke, and D. L. Cooper, Phys. Rev. A **55**, 1064 (1997).

[5] L. Opradolce, R. McCarroll, and P. Valiron, Astron. Astrophys. **148**, 229 (1985).

[6] M. C. Bacchus-Montabonel and P. Ceyzeriat, Phys. Rev. A **58**, 1162 (1998).

[7] H. Tawara, K. Okuno, P. Richard, C. Fehrenbach, C. Verzani, M. P. Stockli, B. Depaola, and P. C. Stancil, Phys. Rev. A (to be published).

[8] Z. Fang and V. H. S. Kwong, Phys. Rev. A **59**, 342 (1996).

[9] R. J. Buenker and S. D. Peyerimhoff, Theor. Chim. Acta **35**, 33 (1974); **39**, 217 (1975); R. J. Buenker, Int. J. Quantum Chem. **29**, 435 (1986). S. Krebs and R. J. Buenker, J. Chem. Phys. **103**, 5613 (1995).

[10] R. J. Buenker, in *Proceedings of the Workshop on Quantum Chemistry and Molecular Physics, Wollongong, Australia*, edited by P. G. Burton (University, Wollongong, 1980); R. J. Buenker, in *Studies in Physical and Theoretical Chemistry*, edited by R. Carbo, *Current Aspects of Quantum Chemistry* (Elsevier, Amsterdam, 1981), Vol. 21, p. 17; R. J. Buenker and R. A. Phillips, J. Mol. Struct.: THEOCHEM **123**, 291 (1985).

[11] G. Hirsch, P. J. Bruna, R. J. Buenker, and S. D. Peyerimhoff, Chem. Phys. **45**, 335 (1980).

[12] M. Larsson, J. Chem. Phys. **86**, 5018 (1987).

[13] A. Veillard, Theor. Chim. Acta **12**, 405 (1968).

[14] W. Meyer and P. Rosmus, J. Chem. Phys. **63**, 2356 (1975).

[15] K. K. Sunil, J. Lin, H. Siddiqui, P. E. Siska, K. D. Jordan, and R. Shepard, J. Chem. Phys. **78**, 6190 (1983).

[16] M. Kimura and N. F. Lane, Adv. At., Mol., Opt. Phys. **26**, 76 (1989).

[17] S. Bashkin and J. O. Stoner, *Atomic Energy Levels and Grotrian Diagrams* (North-Holland, Amsterdam, 1975).

[18] F. J. Smith, Phys. Lett. **20**, 271 (1966).